JOURNAL OF MATERIALS SCIENCE 26 (1991) 4667–4677

Mechanical fatigue of structural ceramics

J. C. GLANDUS
E.N.S.C.I., U.A. C.N.R.S. 320, Avenue Albert Thomas, 87 Limoges, France
QIU TAI
Nanjing Institute of Chemical Technology, People's Republic of China

The mechanical fatigue of structural ceramics has been studied by means of two complementary approaches: numerical simulation of the slow crack growth, and a set of experiments, on polycrystalline alumina. Four loading cases have been considered and the influence of the stress frequency was characterized. The good agreement which was observed between the simulated and the experimental results provides a strong argument for the development of numerical methods in future work.

1. Introduction

The great advantages which may result from the use of ceramics for structural applications have been discussed many times in previous papers, so do not require repetition. All the practical applications envisaged for ceramics exploit their refractoriness and many studies have been published up to now on various mechanical, thermal and chemical topics.

Apart from the particular cases of typically static structures such as heat exchangers, the potential uses of ceramics always concern rotating machines, for example thermal engines or turbines. When operating, these machines induce cyclic mechanical constraints which lead to the failure of components by mechanical fatigue.

In spite of the crucial importance of the failure of ceramic components under mechanical fatigue, there are few papers devoted to this problem, as mentioned by a recent work [1]. Two reasons may be given to explain this: the long duration of experiments and the great scatter in results.

2. Background

The study of the mechanical fatigue of ceramics may be achieved by means of three approaches, eventually complementary. Each of them gives the lifetime of a component on the basis of the validity of the well-known relationship

$$V = AK_1^n \quad (1)$$

in which V is the crack velocity, K_1 the stress intensity factor and n the exponent of propagation.

2.1. Analysis

All the results reported by the literature involve the summation of the elementary lifetime

$$\delta t = \delta a/V \quad (2)$$

along the curve $V = f[(K_1)]$ in which the stress is cyclically dependent on time. (The crack length increases by δa during the time δt.)

2.2. Numerical simulation

An iterative process is used on the basis of the quantification of the lifetime of a component. Each time, for an adjustable time duration during which all the crack propagation parameters are postulated constant, one calculates the crack length, the stress intensity factor, the crack velocity and the resultant increase in crack length. This calculation is repeated until the stress intensity factor reaches the toughness value.

This method of slow crack growth simulation must not be confused with the computerized solutions described in some papers. In these latter cases, a numerical tool is used to calculate the roots of analytical lifetime equations.

2.3. Experiments

In spite of their disadvantages, experiments are needed to validate the results obtained by the two previous methods. We have already underlined their major disadvantages:

(a) Because of the large scatter in the measured lifetime values, many experiments are needed for each experimental condition in order to obtain significant mean results. From this standpoint, it may be noticed that the relations $V = AK_1^n$ and $K_1 = \sigma Ya^{1/2}$, lead to

$$V = A\sigma^n Y^n a^{n/2} \quad (3)$$

and

$$\sigma = K_1 Y^{-1} a^{-1/2} \quad (4)$$

So

$$\delta V/V = (n/2)\delta a/a \quad (5)$$

and

$$\delta\sigma/\sigma = -(1/2)\delta a/a \quad (6)$$

This shows that the instantaneous crack velocities are n times more sensitive to the scatter in initial flaw size than the measured values of strength.

0022–2461/91 $03.00 + .12

(b) The duration of experiments is always very long. This results not only from the scatter in measured lifetime values but also from the need to investigate the range of long lifetimes.

2.4. Discussion

The analytical expression given by the analysis allows the adjustment of many parameters before the calculation of lifetime. Moreover, it is a low cost approach which does not require any previous experiments. Nevertheless, the difficulties arising from calculations may become very significant [2] and, even in the simplest cases, simplifying hypotheses must be postulated.

The numerical simulation is a fully flexible approach which leads to fast calculations of lifetime values. However, the results obtained are strongly dependent on the numerical values chosen for the parameters of the material (A, n, K_{1c}, a, etc.). and, just as for analysis, the hypotheses postulated must be validated.

The experiment presents the disadvantage of a large cost (testing machine and samples) besides those already underlined. On the other hand, it leads to physical lifetime values which involve all the material properties and experimental parameters.

The present study develops two complementary approaches of the mechanical fatigue of ceramics by means of numerical simulation and experiments.

3. Numerical simulation

3.1. Numerical model

The principle of the numerical model used for the present study has been presented in the previous section and it is illustrated by Fig. 1. The program requires, for its initial input, numerical values for the parameters n and $A(V = AK_1^n)$, the toughness K_{1c} and the initial length of the most critical flaw a.

To allow the comparison between the results obtained by simulation and by experiments, the parameters used for simulation are those measured in static fatigue on the material tested in experiments. A previous study [3] gave, $n = 22$, $\ln(A) = -340$ and $K_{1c} = 3.7\ \text{MPa m}^{1/2}$.

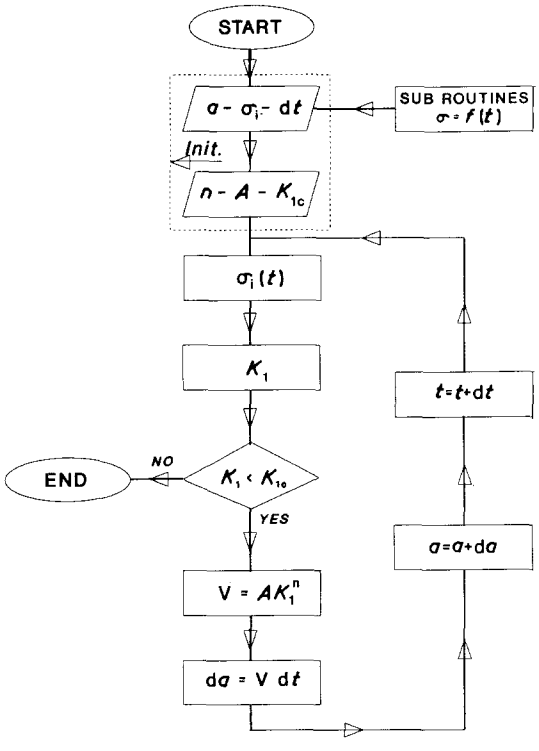

Figure 1 Principle of the program of slow crack growth simulation.

3.2. Reliability of the numerical model

Before calculation of mechanical fatigue lifetimes, the numerical model has been tested in static and dynamic fatigue.

3.2.1. Static fatigue

The lifetime in static fatigue [4] is given by

$$t = 2\sigma_a^{-n}\sigma_c^{(n-2)}/AY^2(n-2)K_{1c}^{(n-2)} \quad (7)$$

so

$$t\sigma_a^n = \text{constant}$$

or

$$\ln(t) = -n\ln(\sigma_a) + \text{constant} \quad (8)$$

Fig. 2 shows that the computed values agree very well with this behaviour: the plot of $\ln(t)$ versus $\ln(\sigma_a)$ is a straight line of slope -22 ($n = 22$) with a regression coefficient equal to -1.000.

The lifetime in static fatigue may also be written

$$t = 2K_{1i}^{(2-n)}/(n-2)A\sigma_a^2Y^2 \quad (9)$$

where K_{1i} represents the stress intensity factor at the beginning of the loading state. But

$$K_{1i} = \sigma_a Y a_i^{1/2} \quad (10)$$

which leads to

$$t = 2(Y\sigma_a a_i^{1/2})^{2-n}/(n-2)A\sigma_a^2Y^2 \quad (11)$$

so

$$t = 2Y^{-n}\sigma_a^{-n}a_i^{(1-n/2)}/A(n-2) \quad (12)$$

or

$$\ln(t) = (1 - n/2)\ln(a_i) + \text{constant} \quad (13)$$

The results given by the numerical model agree again very well with this expression. Fig. 3 shows, indeed, that the slope of the straight line which represents $\ln(t)$ against $\ln(a_i)$ is -10.07 (regression coefficient $r = -1.000$) instead of -10 for $1 - n/2$. Moreover, this figure illustrates the strong influence of the initial crack length on the lifetime. For example, if the crack length increases from 30 to 40 μm, the time to failure decreases in the ratio 1 to 18.

3.2.2. Dynamic fatigue at constant stress rate

In dynamic fatigue [5], the strength depends on the stress rate according to the relationship

$$\ln(\delta\sigma/\delta t) = (n+1)\ln(\sigma) + \text{constant} \quad (14)$$

Fig. 4 confirms that the numerical simulation verifies once more the behaviour of brittle solids: the plot of $\ln(\delta\sigma/\delta t)$ versus $\ln(\sigma)$ is a straight line, the slope of

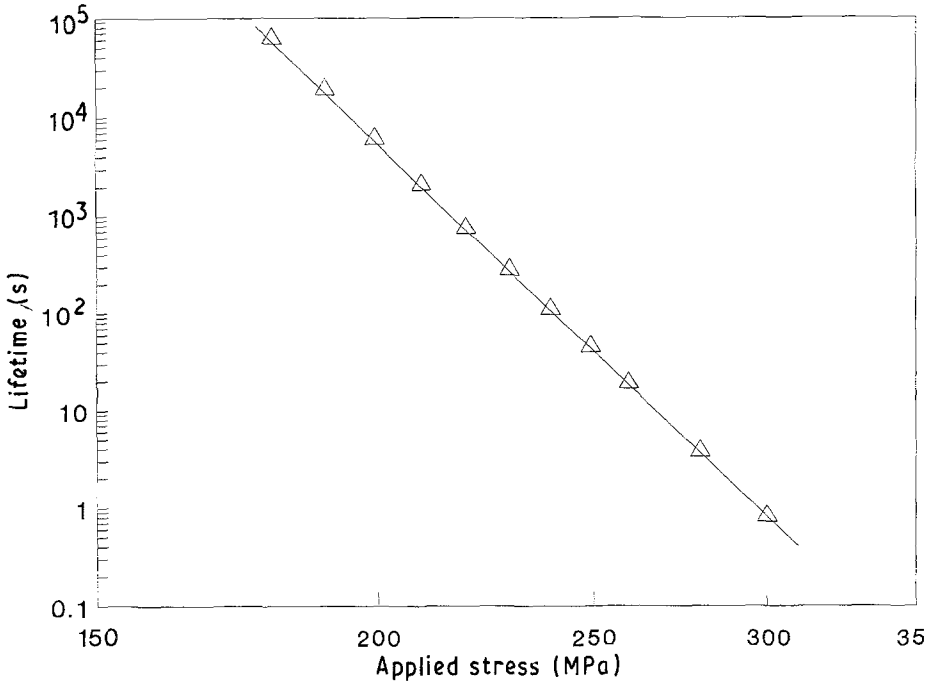

Figure 2 Influence of the applied stress on simulated static fatigue. $n = 22$, $\ln(A) = -340$, $K_{1c} = 3.7\ \text{MPa m}^{1/2}$, initial crack length = 30 μm, slope = 22.

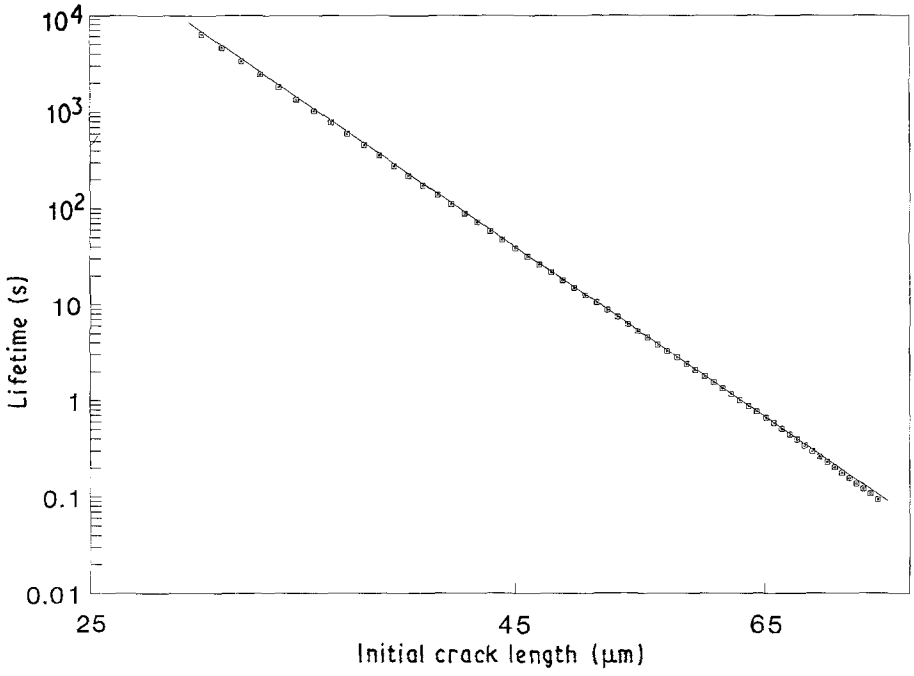

Figure 3 Influence of the initial crack length on simulated static fatigue. $n = 22$, $\ln(A) = -340$, $K_{1c} = 3.7\ \text{MPa m}^{1/2}$, applied stress = 200 MPa, slope = 10.07.

which is 23.3 (regression coefficient $r = 1.000$) whereas $n + 1 = 23$.

3.3. Use of the numerical model

The reliability of the method being obviously established, numerical simulation of the cyclic fatigue can be performed. It has been previously underlined that one of the major interests of the numerical simulation is its flexibility. It allows us to adjust many experimental parameters to simulate various tests. Among the most important of these parameters, one may retain the following.

3.3.1. The frequency

This is one of the prime parameters describing the loading conditions. The program asks for its value at the beginning of each calculation.

3.3.2. The stress time dependence

Sub-routines may be written to simulate various states of stress. For the present study, three common tests have been simulated:

(a) Rotating cyclic fatigue performed on a rotating testing machine (sinusoidal stress time dependence).

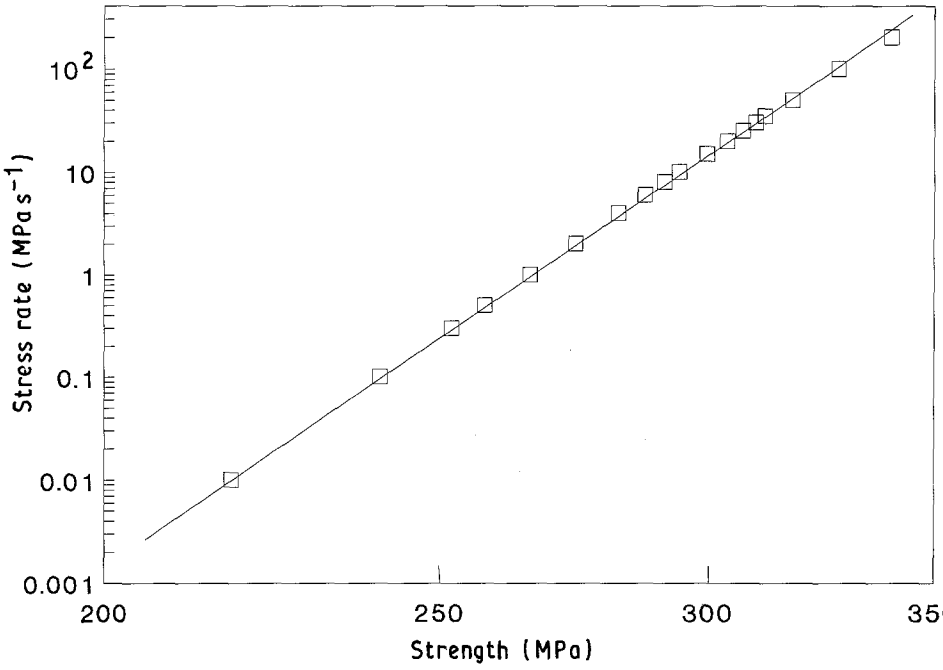

Figure 4 Simulated dynamic fatigue at constant stress rate. $n = 22$, $\ln(A) = -340$, $K_{1c} = 3.7$ MPa m$^{1/2}$, initial crack length = 30 μm, slope 23.3.

(b) Bending cyclic fatigue performed on a soft testing machine (square stress time dependence).

(c) Bending cyclic fatigue performed on a hard testing machine (triangular stress time dependence).

3.3.3. The variations of the r ratio ($r = \sigma_{max}/\sigma_{min}$)

Four experimental cases may be encountered:

(a) σ_{mean} remains constant and $d\sigma$ varies.

(b) σ_{mean} varies and $d\sigma$ remains constant.

(c) σ_{max} remains constant and σ_{min} varies.

(d) σ_{min} remains constant and σ_{max} varies.

$d\sigma$ denotes the stress deviation. ($d\sigma = (\sigma_{max} - \sigma_{min})/2$)

3.4. Results and discussion

All the simulations have been performed with an initial crack length of 30 μm.

3.4.1. First case: σ_{mean} remains constant and $d\sigma$ varies

Loadings with sinusoidal, square and triangular stresses have been simulated with the values of a, n, A and K_{1c} already given. The mean stress is fixed at 180 MPa and the frequency at 1 Hz. Fig. 5 shows the results obtained.

One observes that for similar stress levels, the sinusoidal and triangular stresses lead to comparable lifetime values which are greater than those obtained with square stresses. Moreover, the differences in lifetimes for each case of loading increase when the stress deviation, $d\sigma$, increases. For the limiting case where $d\sigma = 0$, the three loadings lead to the same value: the static fatigue lifetime.

This behaviour is due to the strong dependence (power law) of the crack velocity, V, on the stress intensity factor K_1 (i.e. to the applied stress, σ). So, the greatest stresses are responsible for the major part of

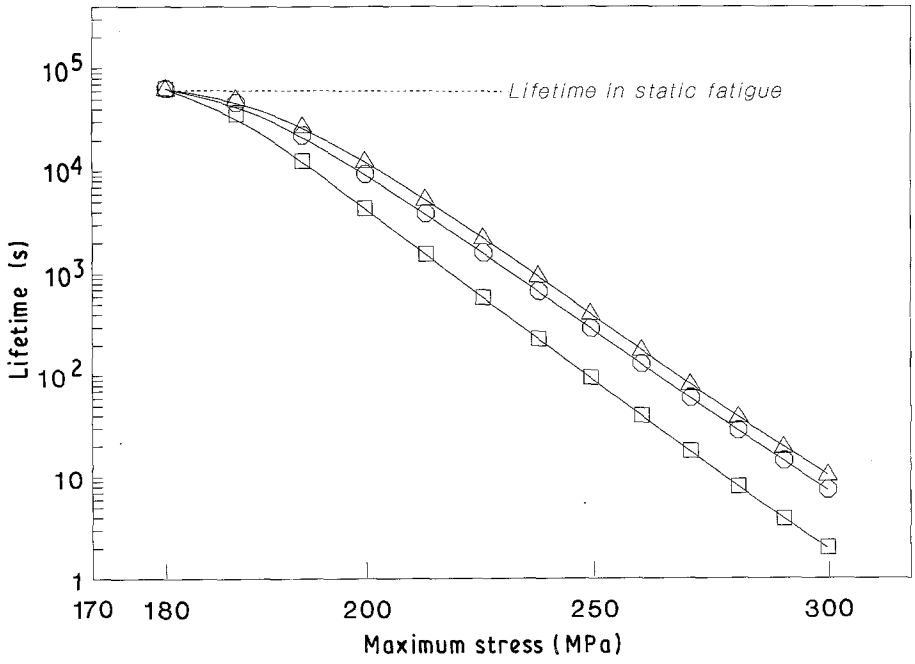

Figure 5 Influence of the stress shape on simulated cyclic fatigue. σ_{mean} remains constant, $d\sigma$ varies. $n = 22$, $\ln(A) = -340$, $K_{1c} = 3.7$ MPa m$^{1/2}$, initial crack length = 30 μm, $\sigma_{mean} = 180$ MPa. (△) Triangular stress, (○) sinusoidal stress, (□) square stress.

the increase in crack length and, therefore, the loadings which maintain the greatest stress level during the longest time lead to the shortest lifetimes.

Finally, one notices that for stress levels greater than 190 MPa, i.e. those for which the loading cannot be considered as static fatigue, the lifetime depends on the maximum stress according to the power law. $N\sigma_{max}^{n'}$ = constant. Such a behaviour, which has been previously observed by means of experiments [6, 7], agrees with the analytical results of Yamauchi *et al.* [8]. However, it differs from the latter study in the n' value which is not strictly equal to the n exponent and which depends on the stress shape:

triangular stress: $n' = 20.17$ ($r = -1.000$)
sinusoidal stress: $n' = 20.18$ ($r = -1.000$)
square stress: $n' = 21.71$ ($r = -1.000$)

The frequency influence on the lifetime has been simulated for the three stress types. Fig. 6 illustrates the results obtained with $a_i = 30\ \mu m$ and $\sigma_{max} = 240$ MPa when A and K_{1c} keep their previous values.

One observes that the lifetime, expressed as the number of endured mechanical cycles, is proportional to the frequency. This means that the lifetime, expressed in units of time, is constant for experimental conditions which differ in frequency values only. The result, established for frequencies ranging from 0.1–40 Hz (i.e. for a frequency ratio of 400) has also been obtained with other initial crack length values and other stress levels. This may be compared with the experimental results of Kröhn and Hasselman [9] who observe, with alumina samples loaded in the ranges 0.1–20 Hz and 5–40 Hz, a slight decrease in the lifetime (in time units) when the frequency increases. Moreover, one may observe again that the loading states which impose the greatest stress levels lead to the smallest numbers of endured mechanical cycles.

3.4.2. Second case: σ_{mean} varies and $d\sigma$ remains constant

Tests of simulation have been performed for hypothetical samples having static fatigue properties identical to those previously used (i.e. $n = 22$, $K_{1c} = 3.7$ MPa $m^{1/2}$, $\ln(A) = -340$ and initial crack length $= 30\ \mu m$). For stress deviations $d\sigma = 10$, 20, 30 and 40 MPa, the influence of the variations of σ_{mean} are illustrated by Fig. 7. One observes that the lifetime depends on the mean stress according to the power law $N\sigma_{mean}^{n^*}$ = constant. The slope, n^*, of the straight lines which represent the variations of $\ln(N)$ versus $\ln(\sigma_{mean})$ decreases in magnitude when $d\sigma$ increases as shown by Table I. It is equal to the exponent of the slow crack growth, n, when $d\sigma = 0$ only. This decrease expresses the fact that, for $d\sigma = 0$, the sample is subjected to static fatigue under the stress σ_{mean} and that the greatest values of $d\sigma$ give rise to the greatest applied stresses. These high stress levels induce high crack velocities which lead to reduced lifetimes. This behaviour has been observed for many other values of the parameters n, a and σ_{mean}.

3.4.3. Third case: σ_{max} remains constant and σ_{min} varies

Keeping the previous material properties constant, five cases of loading have been simulated. The maximum stress has been fixed to 170, 180, 200, 220 and 240 MPa and the minimum stress varies from 1 MPa to the maximum stress value. The expected behaviour is illustrated by Fig. 8 which shows that the lifetime is almost constant up to a σ_{min} level of about 100 MPa. For greater stresses it decreases rapidly and reaches the static fatigue lifetime when the minimum stress

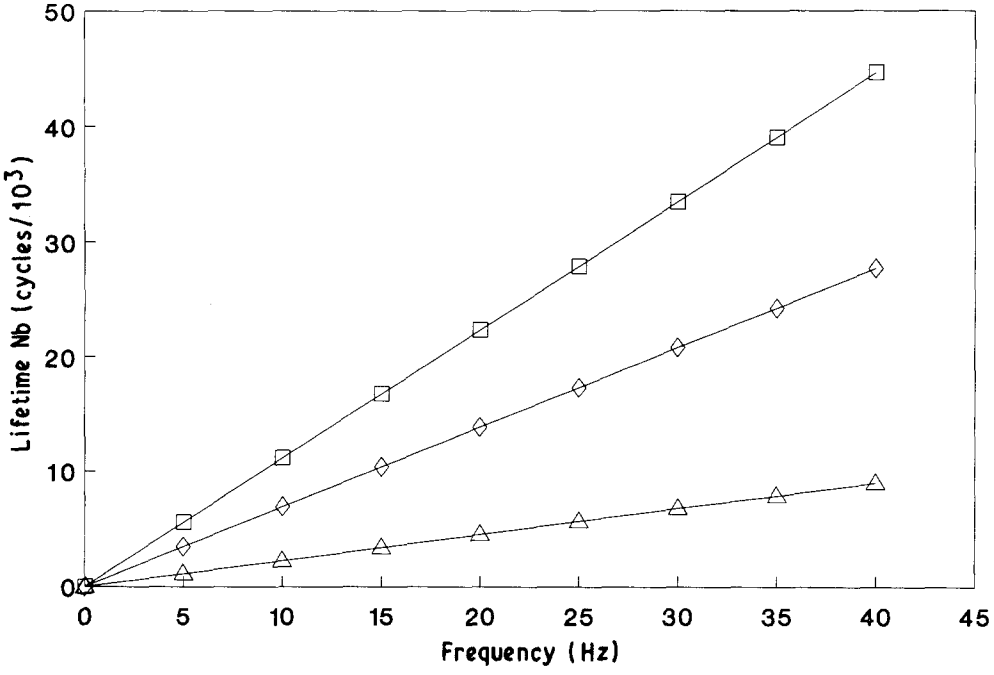

Figure 6 Influence of frequency on simulated cyclic fatigue. $n = 22$, $\ln(A) = -340$, $K_{1c} = 3.7$ MPa $m^{1/2}$, initial crack length 30 μm, $\sigma_{max} = 240$ MPa, $\sigma_{min} = 120$ MPa. (□) Triangular stress, (◇) sinusoidal stress, (△) square stress.

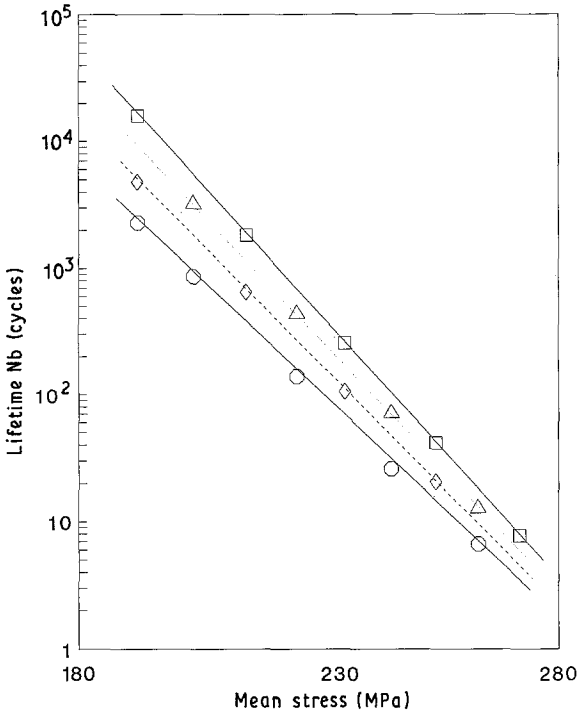

Figure 7 Simulated cyclic fatigue with σ_{mean} variable and $d\sigma$ constant. $n = 22$, $\ln(A) = -340$, $K_{1c} = 3.7$ MPa m$^{1/2}$, initial crack length = 30 μm. $d\sigma$: (○) 40 MPa, slope −18.8; (◇) 30 MPa, slope −19.9; (△) 20 MPa, slope −21.1; (□) 10 MPa, slope −21.7.

TABLE I Slope n^* versus stress deviation $d\sigma$

	$d\sigma$ (MPa)				
	0	10	20	30	40
n^*	22.0	21.7	21.1	19.9	18.8
r	−1.000	−1.000	−1.000	−1.000	−1.000

and the maximum stress are equal. This result illustrates again the strong dependence of the lifetime on the time during which the component is submitted to the greatest stresses.

3.4.4. Fourth case: σ_{min} remains constant and σ_{max} varies

With $\sigma_{min} = 10$, 100, 150 and 170 MPa, four cases of loading have been simulated, for which the maximum stress level ranges from 170–240 MPa. Fig. 9 shows that the lifetime depends on the maximum stress according to the power law $N\ \sigma_{max}^{n^{**}} = \text{constant}$. As found for the second case, the slope, n^{**}, of the straight lines which represent the plots of $\ln(N)$ versus $\ln(\sigma_{max})$ is smaller than the n parameter of the static fatigue. It decreases in magnitude when σ_{min} increases as reported in Table II.

4. Experimental study

4.1. The device

It has already been emphasized that mechanical fatigue tests require numerous samples. Therefore, we have chosen to use samples easy to make and to submit them to simple experiments. Bending tests of prismatic bars were performed at room temperature. An experimental device, allowing the rotation of the bearing rolls (see Fig. 10), has been used to achieve three- and four-point bending measurements in an Instron 1121 universal testing machine. An original counter unit (made in the laboratory), with low and high safety limits, allowed the automatic control of the tests. The crosshead speed was adjusted to ensure a constant frequency of 1 Hz whatever the values of σ_{max} and σ_{min} were.

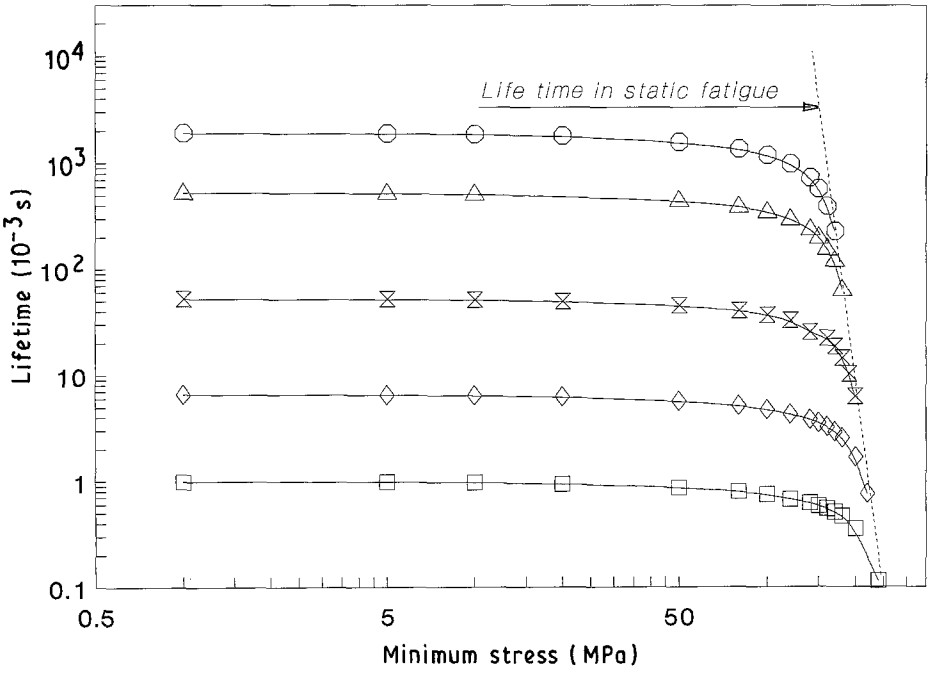

Figure 8 Simulated cyclic fatigue with σ_{max} constant and σ_{min} variable. σ_{max}: (○) 170 MPa, (△) 180 MPa, (⧖) 200 MPa, (◇) 220 MPa, (□) 240 MPa.

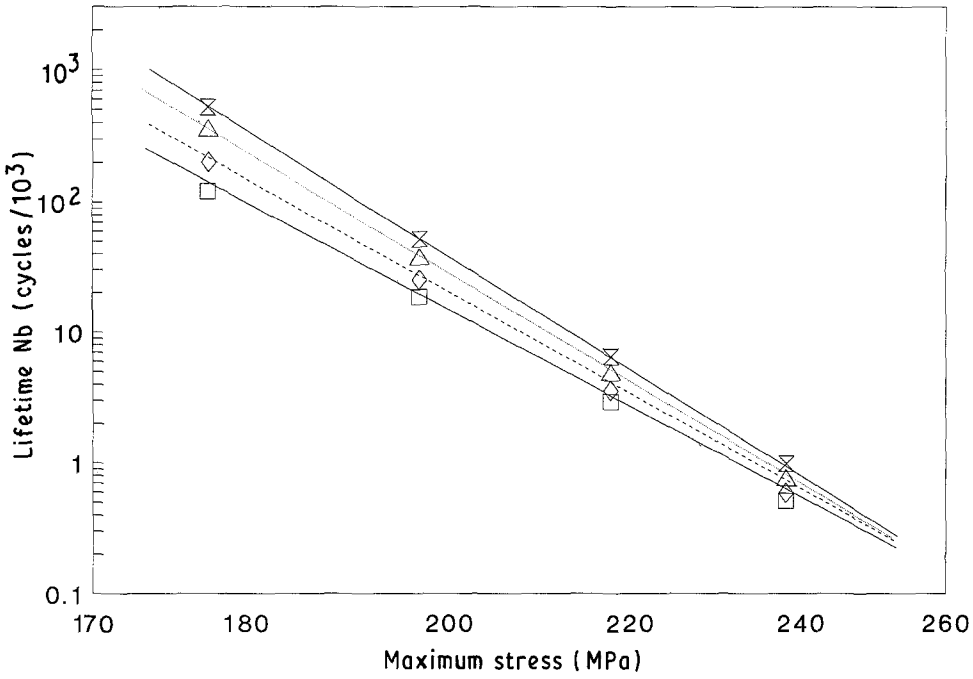

Figure 9 Simulated cyclic fatigue with σ_{min} constant and σ_{max} variable. $n = 22$, $\ln(A) = -340$, $K_{1c} = 3.7\ \text{MPa m}^{1/2}$, initial crack length = 30 μm, σ_{min}: (□) 170 MPa, slope −19.0; (◇) 150 MPa, slope −20.3; (△) 100 MPa, slope −21.4, (⊠) 10 MPa, slope −21.8.

TABLE II Slope n^{**} versus minimum stress level

	σ_{min} (MPa)			
	10	100	150	170
n^{**}	−21.8	−21.4	−20.3	−19.0
r	−1.000	−1.000	−1.000	−1.000

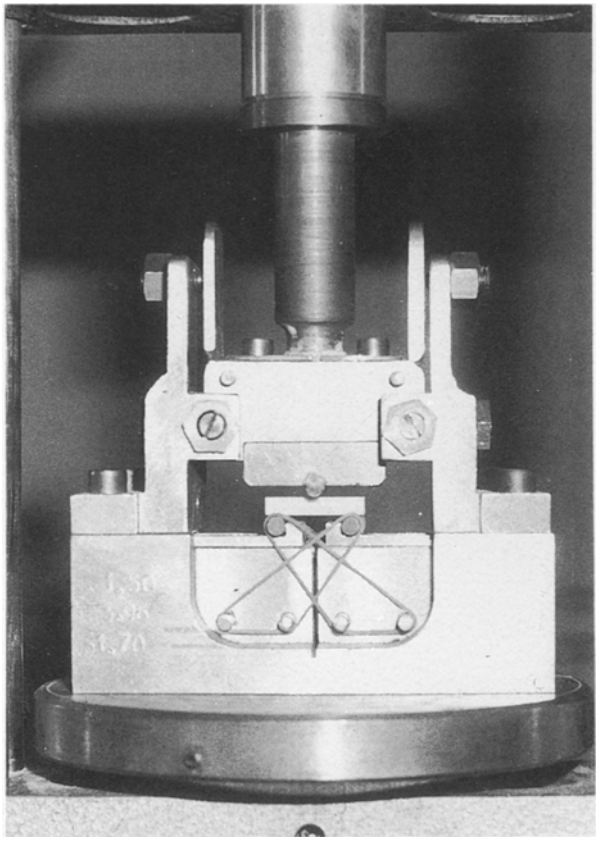

Figure 10 The bending device.

Because the adjustable parameter of the test is the crosshead speed, triangular-shaped stresses are generated.

4.2. Material and samples

A ceramic of commercial quality, the alumina Degussa A123, was used for all the tests. The samples, in the form of prismatic bars 4 mm × 4 mm × 38 mm, were obtained by sawing plates 50 mm × 50 mm × 4 mm. Then they were carefully diamond-polished and their tensile edges were bevelled. The mechanical properties of this material have been previously measured in the laboratory [3, 10] and a set of specific tests have been performed to validate the available data. One of the most important tests confirms, by means of dynamic fatigue at constant stress rate, that the slow crack growth exponent $n(V = AK_1^n)$ is close to 22.

4.3. Results and discussion

Four-point bending tests using polished samples have been firstly carried out because of the uniform stress field induced by such a bending at fixed distance of the neutral fibre. The results obtained were too scattered to be usable. This scatter results from the strong dependence (already emphasized) of the crack velocity on the initial crack length.

To overcome this difficulty, a Vickers indenter has been used to make an artificial flaw crossing the tensile face in the middle of each sample (see Fig. 11). Then, three-point bending tests were performed in order to subject the most critical defect to the greatest stress level. Such a technique has been previously used with success by other authors studying the mechanical fatigue of ceramics [11]. It leads to reasonable scatter in the measured lifetime and sets of 6–8 tests are

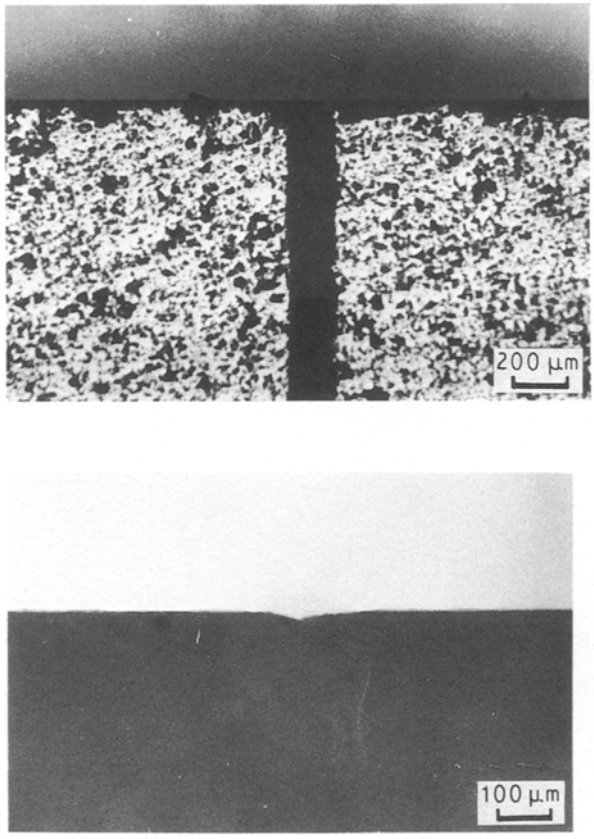

Figure 11 An artificial flow made with a Vickers indenter.

sufficient to give significant mean values for each experimental condition.

4.3.1. *First case:* σ_{mean} *remains constant and* $d\sigma$ *varies*

The mean strength, as measured in three-point bending on samples with an artificial flaw, is 171.5 MPa. Consequently the mean stress for the test is fixed at 100 MPa and the stress deviation $d\sigma$ varies from $\pm$ 20 MPa to $\pm$ 70 MPa.

Fig. 12 shows that the logarithms of the experimental points are well fitted by the straight line. $\ln(N) = -20.1 \ln(\sigma_{max})$, $(r = -0.978)$ or $N_i \sigma_{max}^{20.1} =$ constant, where σ_{max} is the maximum stress value during one cycle. This result, which agrees very well with the relationship found by means of numerical simulation ($N_i \sigma_{max}^{20.17} =$ constant), validates the complementarity of the two approaches developed here. Moreover it confirms that the exponent of cyclic fatigue is not strictly equal to the exponent of static fatigue.

In the previous experimental conditions, the frequency influence has been studied for three frequency values: 0.3, 1 and 3 Hz and four stress levels: $\sigma_{max} =$ 130, 140, 150, 160 MPa. Fig. 13 shows that the behaviour established by simulation is confirmed by experiments. A linear dependence of lifetime on frequency is observed.

4.3.2. *Second case:* σ_{mean} *varies and* $d\sigma$ *remains constant*

Stress deviations of $\pm$ 10 MPa and $\pm$ 20 MPa have been applied to mean stresses varying from 100–150 MPa by steps of 10 MPa. The results are illustrated by Fig. 14 which shows that the lifetime depends on the mean stress according to the power law, $N\sigma_{mean}^{n^*} =$ constant with $n^* = 24.4$ for $d\sigma = \pm$ 10 MPa $(r = 0.985)$ and $n^* = 22.4$ for $d\sigma = \pm$ 20 MPa $(r = 0.983)$. These results are in qualitative agreement with those obtained by simulation. When $d\sigma$ increases, the slope of the straight lines, $\ln(N) = f[\ln(\sigma_{mean})]$, decreases as emphasized by the numerical simulation. However, on the basis of these measured slope values, it may be thought that the value of the slow crack growth exponent is perhaps closer to 24 than to 22.

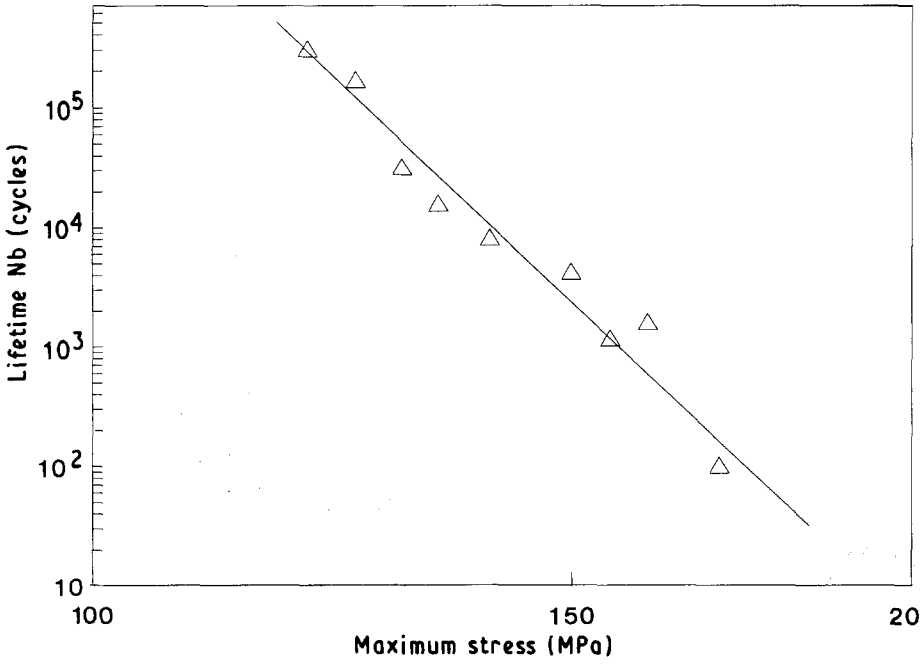

Figure 12 Experimental cyclic fatigue with σ_{mean} constant and $d\sigma$ variable. Mean stress 100 MPa, triangular stress, frequency 1 Hz.

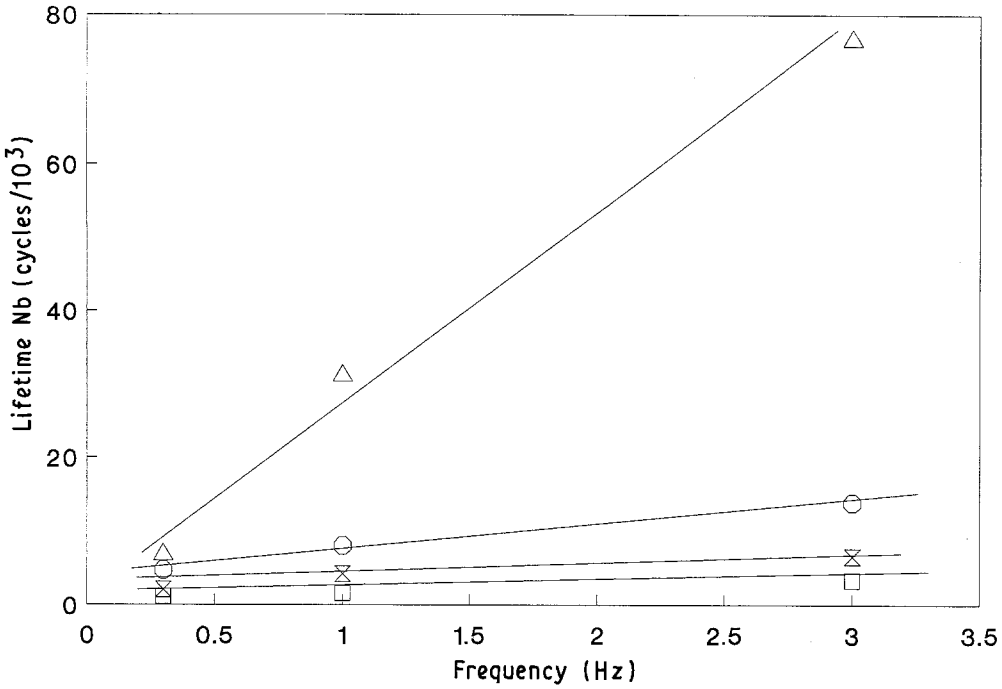

Figure 13 Influence of frequency on experimental cyclic fatigue. σ_{max} (□) 160 MPa, (⊠) 150 MPa, (◇) 140 MPa, (△) 130 MPa.

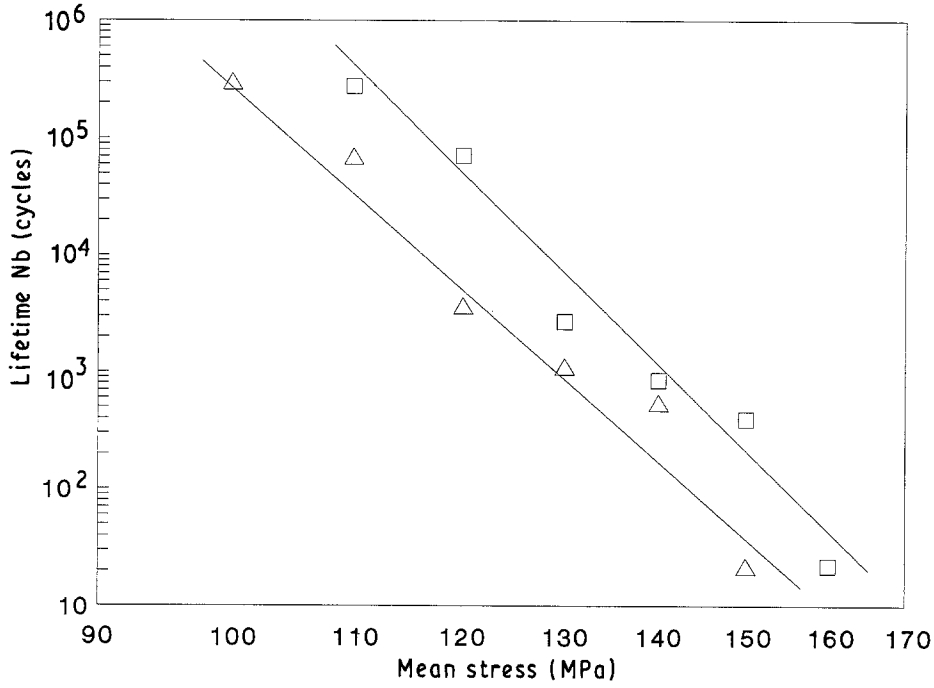

Figure 14 Experimental cyclic fatigue with σ_{mean} variable and $d\sigma$ constant. $d\sigma$: (△) 20 MPa, slope − 22.4, (□) 10 MPa, slope − 24.4.

4.3.3. *Third case: σ_{max} remains constant and σ_{min} varies*

Four sets of experiments have been performed for maximum stress levels fixed at 140, 150, 160 and 170 MPa. The minimum stress ranges from 30–150 MPa. The results are shown in Fig. 15 where straight lines represent the variations of $\ln(N)$ versus $\ln(\sigma_{min})$.

For minimum stress levels ranging from 50 to about 150 MPa, the curves represented in Fig. 8 can be replaced by straight lines, as illustrated by Fig. 16. The slopes of these lines are close to − 1 when σ_{max} is about 170 MPa as observed in experiments. Moreover, experiment as well as simulation leads to the same decrease of this slope when σ_{max} increases. So it may be said that good agreement exists between the simulated and the experimental behaviour.

4.3.4. *Fourth case: σ_{min} remains constant and σ_{max} varies*

Experiments have been carried out for two values of σ_{min}, namely σ_{min} = 70 and 100 MPa. The results are

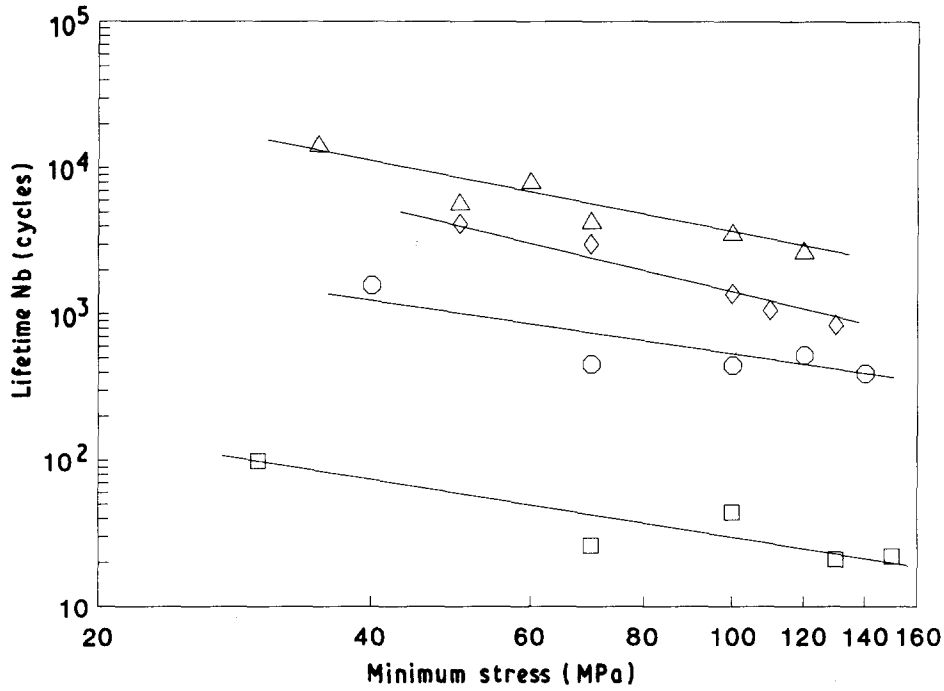

Figure 15 Experimental cyclic fatigue with σ_{max} constant and σ_{min} variable. σ_{max}: (△) 140 MPa, slope − 1.25; (◇) 150 MPa, slope − 1.76; (○) 160 MPa, slope − 0.98; (□) 170 MPa, slope − 0.89.

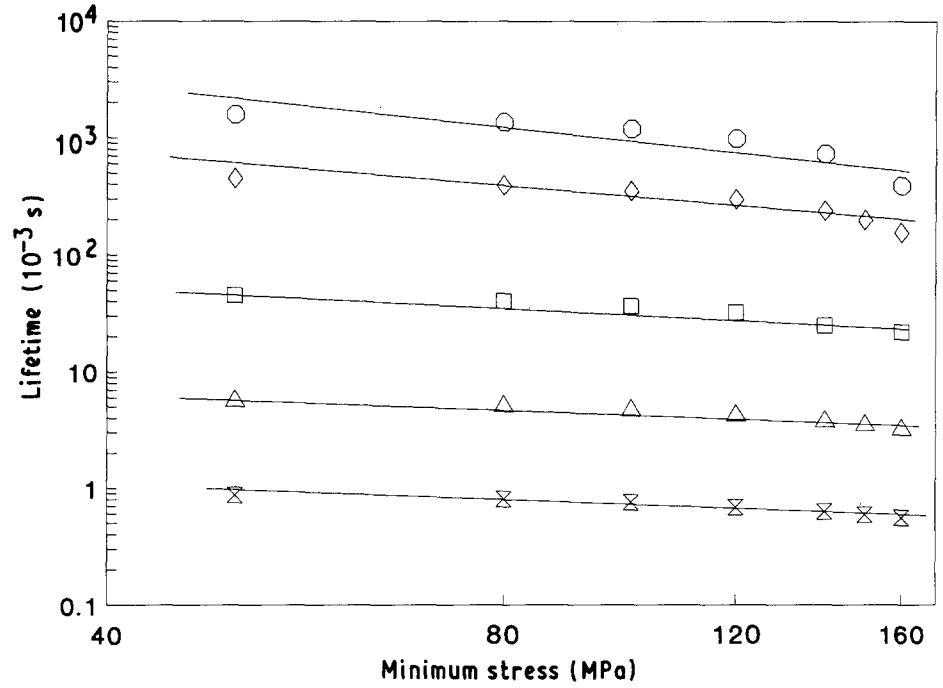

Figure 16 Simulated cyclic fatigue with σ_{max} constant and σ_{min} variable. σ_{max}: (○) 170 MPa, slope − 1.03, (◇) 180 MPa, slope 0.801; (□) 200 MPa, slope − 0.60; (△) 220 MPa, slope − 0.47; (⧖) 240 MPa, slope − 0.39.

illustrated by Fig. 17 which shows again a good agreement between the experimental and simulated behaviour. Because σ_{min} values are too close to distinguish two representative curves, a single straight line is plotted, the slope of which is − 24.5 (r = − 0.981). This value is greater than those given by the method of simulation ($19.02 < n^{**} < 21.80$ when $n = 22$), so it may be thought once more that the exponent of slow crack growth is probably closer to 24 than to 22. It must be recalled that the determination of a reliable numerical value for n is rather difficult, therefore such an uncertainty may be considered as reasonable.

5. Conclusion

An original method of numerical simulation of the slow crack growth has been developed and applied to the case of mechanical cyclic fatigue of structural ceramics. Meanwhile, experiments were carried out on alumina samples subjected to cyclic bending fatigue.

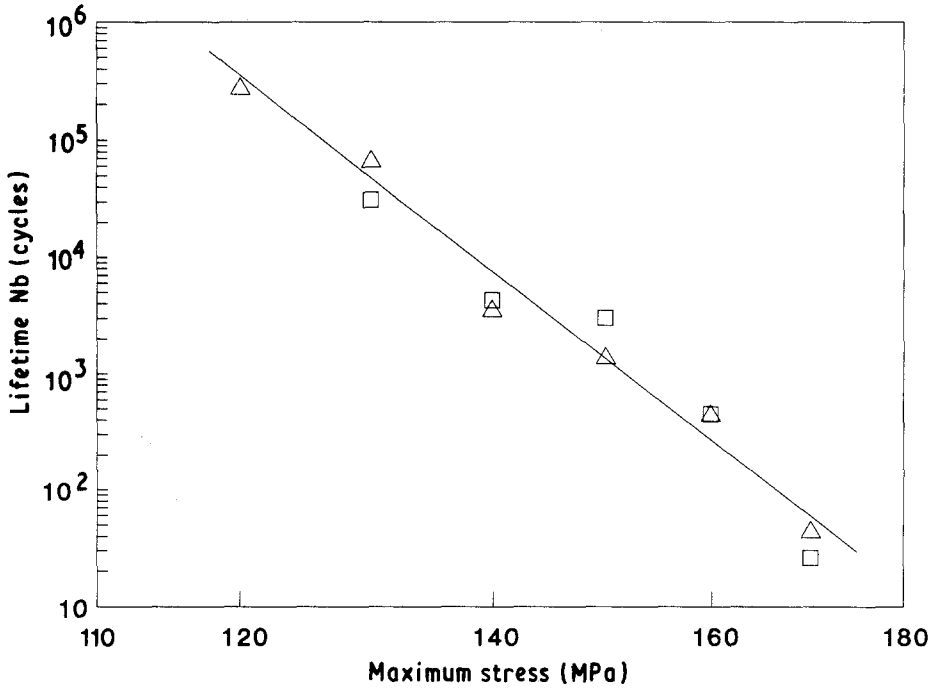

Figure 17 Experimental cyclic fatigue with σ_{min} constant and σ_{max} variable. σ_{min}: (△) 100 MPa, (□) 70 MPa; slope − 24.5.

Four cases of loading have been studied by the two methods and a good agreement was observed between the results given by each of them. Moreover, the dependence of lifetime on both the stress frequency and the stress shape has been established.

The obvious complementarity of these techniques emphasizes the great interest of the numerical simulation method. The use of this tool allows the reduction of the number of mechanical tests and leads therefore to a significant decrease in the duration of material studies.

References

1. F. SCAFARTO, E.N.S.C.I. Internal Report, Limoges (1988).
2. A. G. EVANS and E. R. FULLER, *Metall. Trans.* **5** (1974) 27.
3. J. P. BROUSSE, C.N.A.M. Report, University of Limoges, Limoges (1981).
4. R. W. DAVIDGE, *Ceram. Int.* **1** (1975) 75.
5. J. E. RITTER Jr *et al. J. Amer. Ceram. Soc.* **62** (1979) 542.
6. T. FETT *et al. Adv. Ceram. Mater.* **1** (1986) 179.
7. S. CHO *et al. J. Mater. Sci. Lett.* **6** (1987) 801.
8. Y. YAMAUCHI *et al.* Proceedings of the 27th Japanese Congress on Materials Research (1984) p. 235.
9. D. A. KRÖHN and D. P. H. HASSELMAN, *J. Am. Ceram. Soc.* **55** (1972) 208.
10. J. C. GLANDUS, PhD Thesis, University of Limoges, Limoges (1981).
11. T. KAWAKUBO and K. KOMEYA, *J. Amer. Ceram. Soc.* **70** (1987) 400.

Received 22 January
and accepted 30 October 1990